sustainability

Article

Maximum Power Point Tracking of a Grid Connected PV Based Fuel Cell System Using Optimal Control Technique

Muhammad Majid Gulzar

Control & Instrumentation Engineering Department & Center for Renewable Energy and Power Systems, King Fahd University of Petroleum & Minerals, Dhahran 31261, Saudi Arabia; muhammad.gulzar@kfupm.edu.sa

Abstract: The efficiency of renewable energy sources like PV and fuel cells is improving with advancements in technology. However, maximum power point (MPP) tracking remains the most important factor for a PV-based fuel cell power system to perform at its best. The MPP of a PV system mainly depends on irradiance and temperature, while the MPP of a fuel cell depends upon factors such as the temperature of a cell, membrane water content, and oxygen and hydrogen partial pressure. With a change in any of these factors, the output is changed, which is highly undesirable in real-life applications. Thus, an efficient tracking method is required to achieve MPP. In this research, an optimal salp swarm algorithm tuned fractional order PID technique is proposed, which tracks the MPP in both steady and dynamic environments. To put that technique to the test, a system was designed comprised of a grid-connected proton exchange membrane fuel cell together with PV system and a DC-DC boost converter along with the resistive load. The output from the controller was further tuned and PWM was generated which was fed to the switch of the converter. MATLAB/SIMULINK was used to simulate this model to study the results. The response of the system under different steady and dynamic conditions was compared with those of the conventionally used techniques to validate the competency of the proposed approach in terms of fast response with minimum oscillation.

Keywords: renewable energy sources; fuel cell; photovoltaic; maximum power point; fractional order PID

Citation: Gulzar, M.M. Maximum Power Point Tracking of a Grid Connected PV Based Fuel Cell System Using Optimal Control Technique. *Sustainability* **2023**, *15*, 3980. https://doi.org/10.3390/su15053980

Academic Editor: Elena Cristina Rada

Received: 16 December 2022
Revised: 17 January 2023
Accepted: 15 February 2023
Published: 22 February 2023

1. Introduction

Conventional energy sources are being depleted at an alarming speed and becoming scarce; thus, the usage of unconventional energy sources is growing. Coal, petroleum, natural gas, and nuclear power are all major conventional sources. Because of their continued use, these resources have been exhausted to a great extent. Additionally, the usage of these sources contributes significantly to pollution, which contributes to global warming. Owing to these issues, scientists are forced to employ renewable energy sources (RES). Non-conventional/RES are sources of energy that are reproduced by natural processes regularly and do not deplete [1]. These sources do not damage our environment, are mostly cost-effective, and often do not require a huge investment, hence widely being accepted as more reliable. Moreover, these sources are called renewable because they are renewed or reproduced at an equal or greater rate with respect to the rate of their use.

Among all RES, solar PV, which utilizes the photovoltaic effect to produce electricity, is being widely used worldwide. Sunlight is absorbed using semiconductor materials—mostly silicon—and converted into electrical energy. The foremost drawback of solar energy is that a large area is required to install solar PV systems [2,3]. The fuel cell is, in fact, a device (electro-chemical) that uses a chemical reaction to produce electrical energy [4]. A fuel cell utilizes the energy of hydrogen (chemical energy) or other fuels to generate electricity in a clean and effective manner. When hydrogen is utilized as a fuel, the only things created are heat, electricity, and water. The prominent and unusual aspect of fuel cells is that they can be used for an extensive range of applications [5,6].

Fuel cells and batteries differ significantly from each other, as fuel cells do not require recharging since they do not run out of fuel. The fuel cell will keep producing heat and power until the fuel supply stops. A fuel cell is constructed using two electrodes sandwiched around an electrolyte. In a fuel cell, the anode is the negative $(-)$ electrode while the cathode is the positive $(+)$ electrode. Hydrogen is widely used as fuel in fuel cells and is provided to the anode [7], while the oxygen (from the air) is supplied to the cathode. A catalyst is needed to initiate the redox reaction. Platinum is used as a catalyst and, in some cases, enzymes are used. The catalyst converts hydrogen into electrons and protons (hydrogen ions). Here, electrons take an exterior circuit path and can be utilized to power a load, while protons cross through the electrolyte to combine with oxygen to form water [8].

Several classifications of fuel cells are currently under research, each using different fuels with different electrochemical reactions and construction. Each has a different catalyst requiring different operating conditions like temperature and has its own applications and drawbacks. Polymer Electrolyte Membrane Fuel Cells (PEMFC), also identified as proton exchange membrane fuel cells, provide a higher power density than other traditional fuel cells while being lighter in weight and smaller in size [9,10].

One vital aspect of the PV based fuel cell is tracking its maximum power point (MPP). For reliable and efficient use, it is important to use a PV based fuel cell at MPP, which depends on several factors, including irradiance, temperature, water content in membrane, and hydrogen and oxygen partial pressures. The Perturb and Observe (P&O) algorithm is the most popular to track MPP, owing to its simplicity. However, it may cause fluctuations across MPP due to excessive switching. To reduce these fluctuations, the step size can be reduced; but this will cause the tracking time to increase. The incremental conductance method is proposed in [11,12], which gives better results than the P&O, but still causes an overshoot. Sliding mode controller (SMC) is studied in [13], using a fuel cell stack with a boost converter, and performance is compared with incremental conductance and P&O. However, while it yields a significantly lower overshoot, the calculations are extensive and the design of the filter is difficult.

The Water cycle algorithm (WCA) is an effective algorithm to track MPP and it is inspired by the naturally occurring water cycle. The drawback of WCA is that it can trap in local optima [14]. The incremental conductance method has been implemented for MPP tracking, but its implementation is complex as it requires multiple sensors [15]. The author in [16] suggested a smart drive algorithm using a boost converter to track the MPP of the fuel cell, but the efficiency of the method turned out to be less than other metaheuristic techniques. Particle swarm optimization (PSO) is another technique used for MPP tracking, which is based on the natural process. Ref [17] discussed the PSO technique using a fuel cell stack with a boost converter. PSO is a metaheuristic approach, but the drawback is that it can also be stuck in local optima. Extremum seeking control is an efficient method but converges slowly [18].

A fuel cell model with a cuke converter is discussed in [19] and the firefly algorithm (FFA) is proposed to reach MPP. FFA is a metaheuristic technique, but it has a drawback, namely, in that it may be stuck in local optima. Backstepping techniques proposed in [20], show good efficiency, but the implementation requires great effort as it is very complex. Fuzzy logic control (FLC) is another important technique used to track MPP and is being used widely. FLC has been implemented using both Boost and Buck converters. The accuracy of FLC is low and one cannot be sure that the MPP calculated by the controller is accurate [21,22]. Convergence time for FLC, if used independently, can be very large. Another technique proposed in [23] is an artificial neural network (ANN); however, this technique requires an excessive amount of data.

A Jaya controller with cuke converter is implemented in [24] to improve MPP. The presented technique is metaheuristic but requires excessive computational time. The grey wolf optimization (GWO) method is also introduced in [25] to track MPP. GWO technique is motivated by the leadership hunting and hierarchy methodology of grey wolf packs. GWO is a metaheuristic technique, but its convergence rate is slow and it can be stuck in local optima. Another nature-inspired optimization technique is the salp swarm optimization (SSO) algorithm which is discussed in [26]. Despite being metaheuristic, it requires excessive computational time for processing. Anti-windup PID controllers are being used commonly in industries, due to their simplicity and fewer computational requirements [27]. However, PID is sensitive to excessive variations and can lead a system to instability. Moreover, it cannot be used for non-linear systems [28].

Higher-order sliding mode controllers tuned with a twisting algorithm (HOSM-TA) are implemented in [29]. They show high robustness against disturbances and uncertainties. The drawback of this technique is that it is very complex and there is no guarantee that the solution is accurate. Furthermore, it cannot be used for 1st order systems. Chattering is a phenomenon that decreases the efficiency of SMC and also causes heat loss in the system. To overcome this, a Quasi-continuous (QC) algorithm is proposed in [30]. This proposed technique shows considerable improvement against chattering and is also robust. Nonetheless, one of the major drawbacks is that it is complex in design with no guarantee of accuracy, and cannot be used for 1st order systems. Higher-order prescribed convergence law technique (PCL) is used to track MPP using a DC-DC boost converter, which is a robust technique and has a finite convergence time, but it is also complex with low accuracy [31]. Another MPP tracking technique is model predictive control (MPC), which offers multiple variable control and predicts upcoming disturbances and upcoming control actions. It is better than many other techniques in terms of energy savings and has enhanced transient response, but it requires specific background knowledge of the method to be implemented [32,33]. Tuning of PID with SSO technique shows good results with reasonable execution time and good accelerated convergence, and requires few parameters to be tuned [34]. However, it can suffer from premature convergence.

The integral fast terminal sliding mode control (IFTSMC) technique has advantages, e.g., robustness against uncertainties and disturbances, ability to reduce chattering, and high speed of convergence [35]. The golden section search technique is another technique for MPP. Although this technique is faster than many heuristic methods, the implementation of the same can be costly; furthermore, it requires knowledge of fuel cell plant specifications [36]. The forensic-based investigation algorithm (FBI) has been used for proportional integral derivative, which requires multiple sensors and, hence, can be costly [37]. The equilibrium optimizer algorithm is adopted to optimize FLC for MPPT. The algorithm itself is complex and also FLC lacks in accuracy [38,39].

Table 1 lists the key characteristics and provides a comparison of the various approaches previously employed.

Table 1. Summary of Fuel Cell-based MPPT Techniques.

Sr. #	Reference #	Algorithm/ Approach	Converter Type	Nature/Remarks/Notes
1	[5]	IC	Boost	Multi-sensors are required
2	[6]	PSO	Boost	Easily trapped in local optimum
3	[7,8]	ANFIS	Boost	ANN requires excessive data
4	[9]	P&O	High step ratio	Oscillations/fluctuations near MPP with large tracking time
5	[10]	MPC	Boost	Requires plant model and specific knowledge
6	[11,12]	P&O/InC	Buck	Oscillations/fluctuations near MPP multi-sensors needed

Table 1. *Cont.*

Sr. #	Reference #	Algorithm/Approach	Converter Type	Nature/Remarks/Notes
7	[13]	SMC	Boost	The design of the filter circuit is cumbersome
8	[14]	WCA	Boost	It may become stuck in local optima
9	[15]	INR	Boost	Multiple sensors are needed
10	[16]	Smart drive algorithm	Boost	Low accuracy
11	[17]	PSO	Boost	Easily stuck in local optima
12	[18]	Extremum seeking control	-	Slow convergence rate
13	[19]	Firefly algorithm	Cuke	Easily trapped in local optimum
14	[20]	Backstepping	Boost	Complex/Excessive effort in implementation
15	[21]	Fuzzy logic	Boost	Lacks precision
16	[22,23]	ANN	Boost	ANN requires excessive data
17	[24]	Jaya	Cuke	Requires Excessive computational time
18	[25]	GWO	Boost	Sluggish convergence and stuck in local optimum
19	[26]	SSA	Boost	Excessive computational time required
20	[27]	AW-PID	Buck-Boost	Inefficient and sensitive toward large load changings and not suitable for Nonlinear systems
21	[28]	FPID	Four switch Buck-Boost	Complex to implement
22	[29]	TA	Boost	Complex and accurate results not guaranteed
23	[30]	PCL	Boost	High complexity and low accuracy
24	[31]	QC	Boost	Cannot be used for 1st order systems, complex and less accurate
25	[32]	MPC	Two-level inverter	Requires plant model and specific knowledge
26	[33]	MPC	Boost	Requires plant model and specific knowledge
27	[34]	SSA-PID	Boost	Can become stuck in the local maximum

Table 1. *Cont.*

Sr. #	Reference #	Algorithm/ Approach	Converter Type	Nature/Remarks/Notes
28	[35]	IFTSMC	Boost	Knowledge of system boundary uncertainty is required, also convergence issues when states are not near equilibrium.
29	[36]	GSS	Boost	Implementation cost high and knowledge of plant specification of the fuel cell required
30	[37]	FBI-PID	Boost	Multiple sensors required, hence costly
31	[38]	EO-FLC	Boost	Fuzzy logic may lack in accuracy

Novelty and Contribution

The literature review reveals specific areas that need further improvement; thus, the proposed technique has focused its utility on these areas. This main contribution of the proposed work is as follows:

1. This work presented an optimum salp swarm algorithm tuned fractional order PID controller for MPPT to modify input and output during transient operating conditions to attain an ideal duty ratio.
2. Compared to other traditional MPPT algorithms utilized in the literature, it offers high-power tracking capability, quick convergence speed, fewer controlling parameters, and ease of implementation.
3. The PV-based fuel cell grid connected technology offers a guarantee for steady and practical operation under varying load situations.

The paper is organized as follows. Section 2 provides the design and modeling of the PV and Fuel Cell. The proposed control strategy is described in Section 3. Section 4 is designated for the attained results and discussions. Section 5 is dedicated to the conclusion.

2. System Modeling

The system under study is designed to comprise a grid-connected proton exchange membrane fuel cell (PEM) together with PV system, a DC-DC boost converter along with resistive load, and a robust power point tracking controller. The output from the controller is further tuned and PWM is generated, which is fed to the switch of the converter. Figure 1 presents an overview of the model under study.

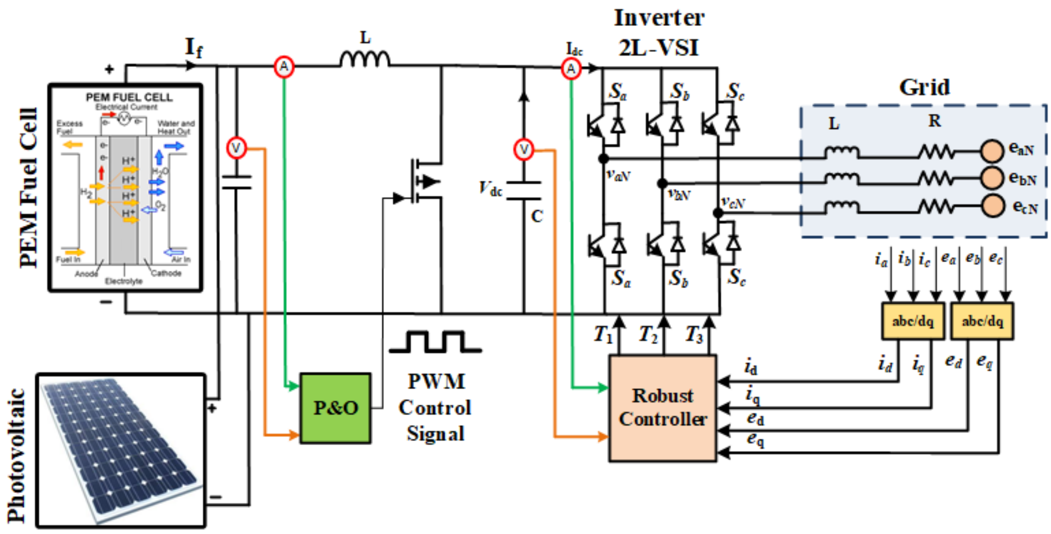

Figure 1. Fuel cell and PV to Grid stages.

2.1. Fuel Cell System Modelling

Fuel cells, first conceived by Sir William Grove in 1839, are now a viable source of energy. Fuel cells may be thought of as generators in their most basic form. Unlike traditional generators, which utilize internal combustion engines to turn an alternator, fuel cells create electricity by directly creating electrons with no moving components. As a result, they are quite effective and dependable. They are also almost silent, producing only water vapor in addition to energy and heat. As a result, they are suitable for indoor usage.

The voltage-current characteristics of fuel cells are intricate and nonlinear. A polarization curve illustrates the non-linear connection between a fuel cell's current density and voltage. The fuel cell output voltage is controlled by current density, which is affected by operational parameters. A PEMFC, a boost DC/DC converter, as well as a resistive load make up the system. The controlling variable within that system is the duty cycle of the boost converter; which is the driving variable for achieving MPPT, where C and L stand for the capacitance and inductance of the boost converter, respectively.

The fuel cell output is given by Equation (1)

$$V_{cell} = E_{Nernst} - V_{act} - V_{ohm} - V_{conc} \tag{1}$$

where E_{Nernst} is reversible thermos-dynamic potential which is defined by Nernst Equation (2)

$$E_{Nernst} = 1.229 - 8.5 \times 10^{-4}(T - 298.15) + 4.308 \times 10^{-5}T\left(\ln(P_{H_2} + 0.5\ln(P_{o_2})\right) \tag{2}$$

where T indicates the absolute temperature in kelvins, P_{H_2} is hydrogen partial pressure (atmospheric) and P_{o_2} is the oxygen partial pressure. Activation voltage drop is given by Tafel Equation (3)

$$V_{act} = \zeta_1 + \zeta_2 T + \zeta_3 T \ln(C_{o_2}) + \zeta_4 T \ln(\mathrm{I}_{FC}) \tag{3}$$

Here $i = 1, \ldots, 4$ are parametric coefficients for every cell model, and C_{o_2} denotes the dissolved-oxygen concentration in the interface of the cathode catalyst, as mentioned in Equation (4)

$$C_{o_2} = \frac{P_{o_2}}{(5.08 \times 10^6) \times \exp\left(-\frac{498}{T}\right)} \tag{4}$$

The overall ohmic voltage drop is calculated as Equation (5)

$$V_{ohm} = \mathrm{I}_{FC}\mathrm{R}_M \tag{5}$$

where R_M is the resistance (ohmic) and is made up of the electrode resistances as well as the resistances of the polymer membrane and electrodes. Here, R_M is provided by Equation (6)

$$R_M = \frac{r_m\, t_m}{A} \tag{6}$$

where, t_m is the membrane thickness, which is in centimeters, A is the activation area in micro centimeters, and r_m is the membrane resistivity Ωcm to proton conductivity. Membrane humidity and temperature have a significant impact on membrane resistivity, which can be computed as Equation (7)

$$r_m = \frac{181.6\left[1 + 0.03\left(\frac{I_{FC}}{A}\right) + 0.0062\left(\frac{T}{303}\right)^2\left(\frac{I_{FC}}{A}\right)^{2.5}\right]}{\left[\lambda_m - 0.634 - 3\left(\frac{I_{FC}}{A}\right)\right] \times \exp\left(4.18\left(T - \frac{303}{T}\right)\right)} \tag{7}$$

where, water content is represented by λ_m of the membrane and is an input of the PEMFC model. In addition, it is a function of the average water activity a_m as represented in Equation (8)

$$\lambda_m = \left\{\begin{matrix} 0.043 + 17.81a_m - 39.85a_m^2 + 36a_m^3 \; 0 < a_m < 1 \\ 14 + 1.4(a_m - 1) \; 1 < a_m \leq 3 \end{matrix}\right\} \tag{8}$$

The relationship between the average water activity and the anode and cathode water vapor partial pressures, ($P_{v,an}$, $P_{v,ca}$ respectively) is given by Equation (9)

$$a_m = \frac{1}{2}(a_{an} + a_{ca}) = \frac{1}{2}\left[\frac{P_{v,an} + P_{v,ca}}{P_{sat}}\right] \tag{9}$$

The saturation pressure of water P_{sat} can be calculated with the subsequent empirical expression as mentioned in Equation (10)

$$\mathrm{lpg}_{10}P_{sat} = -2.1794 + 0.02953T - 9.1813 \times 10^{-5}T^2 + 1.4454 \times 10^{-7}T^3 \tag{10}$$

The values (real-time) of λ_m can vary from 0 to 14. The concentration voltage drop is expressed as Equation (11)

$$V_{conc} = -\frac{RT}{nF}\ln\left(1 - \frac{i_{FC}}{i_L A}\right) \tag{11}$$

where, i_L is the limiting current and it is the maximum rate at which the reactant may be given to an electrode.

Fuel cells are linked together in a series to produce the desired voltage. Thus, the N_{FC} series cells per string have nonlinear $V - I$ characteristics, as mentioned in Equation (12)

$$V_{FC} = N_{FC}V_{cell} \tag{12}$$

2.2. PV System Modelling

The PV system is one of the most extensively used RES. The current source is parallel to the diode and precisely converts solar energy into electrical energy by accelerating the flow of holes and electrons inside the photovoltaic cell. It is required to create the PV source to unavoidably operate on its MPPT in order to get maximum power, since it is a non-linear current source [40].

A PV array needs to go through a number of processes to connect with a thermal power supply. As demonstrated in Figure 2, the design of a PV system includes a number of components, including a converter, an inverter, modeling, and a computation of the average power that is actually sent to the grid.

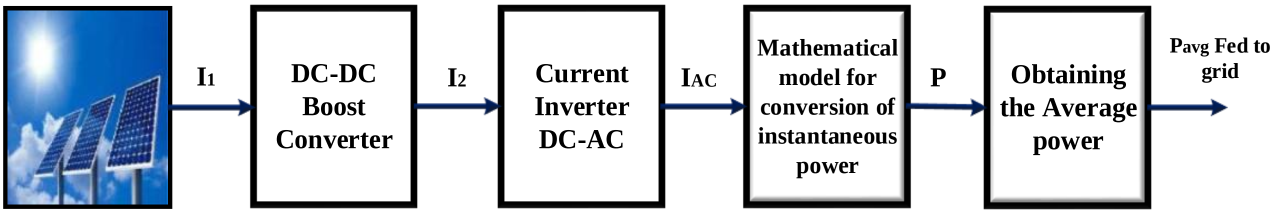

Figure 2. Grid Connected PV Farm Prototype.

AC voltage of PV can be calculated, by using Equation (13).

$$q = \frac{v_{dc}}{v_{ac}} \tag{13}$$

Here q is the gain between AC-DC voltage. The boost converter transfer function (TF) can be projected using Equations (14) and (15)

$$m_1 = \frac{v_2}{v_1} = \frac{i_1}{i_2} \tag{14}$$

$$g_1(s) = \frac{1}{m_1} \tag{15}$$

where $\frac{1}{m_1}$ is the boost converter gain. The inverter TF is mentioned in Equation (16)

$$g_2(s) = \frac{I_{ac}(s)}{I_2(s)} = \frac{s^2}{s^2 + \omega^2} \tag{16}$$

Here, $\omega = 2\pi f = 2\pi(50) = 314.12\text{rad/s}$. For instantaneous power, the TF is mentioned in Equation (17), where $\frac{v_m}{i_m}$ is the impedance.

$$P(s) = \frac{v_m i_m}{2s} + \frac{v_m i_m}{2} \frac{s}{s^2 + (2\omega)^2} \tag{17}$$

The instantaneous power gain is given in Equation (18)

$$g_3(s) = \frac{p(s)}{I_{ac}(s)} = v_m \left(\frac{\left(s^2 + \omega^2\right)\left(s^2 + (2\omega)^2\right)}{s^2(s^2 + (4\omega)^2)} \right) \tag{18}$$

The average power is mentioned in Equation (19)

$$p_{avg}(s) = \frac{v_m i_m}{2s} \tag{19}$$

The average power gain is shown in Equation (20)

$$g_4(s) = \frac{p_{avg}(s)}{p(s)} \tag{20}$$

3. Proposed Robust Controller

The proposed robust controller is a combination of the Salp Swarm Algorithm tuned Fractional order PID controller to achieve the MPPT of the hybrid PV based fuel cell system, as shown in Figure 3.

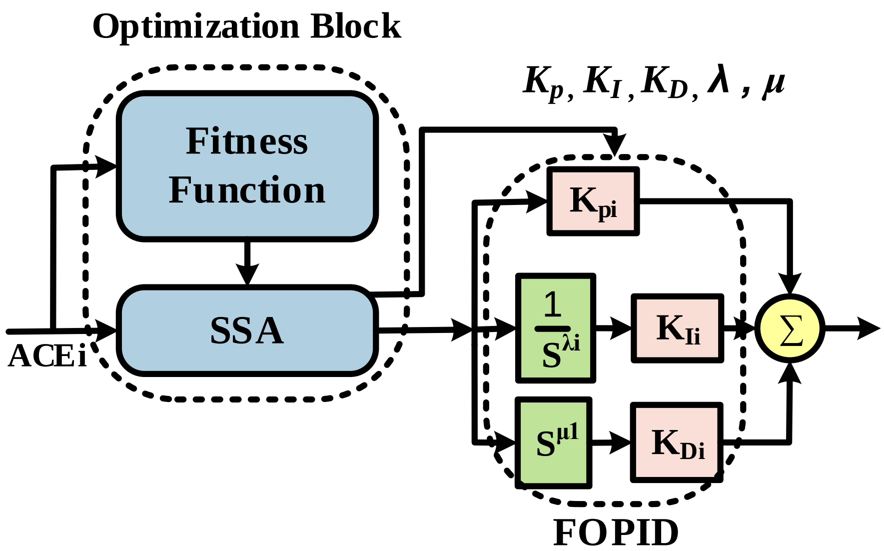

Figure 3. Proposed Robust Controller.

3.1. Salp Swarm Algorithm

The method is inspired by transparent body salp vertebrates, which are famous for generating spiral chains when they travel to find food [41]. The leader and followers are the two basic divisions of the salp swarm. The leader's role is to direct the group as they look for food, and they update their position using Equation (21)

$$K_j^i = \begin{Bmatrix} M_i + C_1\big(\big(ub_j - lb_j\big)C_2 + lb_j\big)\ C_3 \geq 0 \\ M_i - C_1\big(\big(ub_j - lb_j\big)C_2 + lb_j\big)\ C_3 < 0 \end{Bmatrix} \tag{21}$$

Here, lb_j and ub_j stands for the lower and upper limits of the j^{th} dimension, while M stands for the target food and K is the $2D$ salp position. The variables C_2 and C_3 are uniform coefficients. The C_1, which is shown in Equation (22), is utilized to balance the exploitation of food in search space.

$$C_1 = 2e^{-\left(\frac{4t}{t_{max}}\right)^2} \tag{22}$$

where t and t_{max} denotes the current and maximum iterations, respectively. Equation (23) is used to update the position of the follower salp.

$$K_j^i = \frac{1}{2}at^2 + v_0 t\ i \geq 2 \tag{23}$$

The flow chart of the complete Salp Swarm Algorithm is depicted in Figure 4.

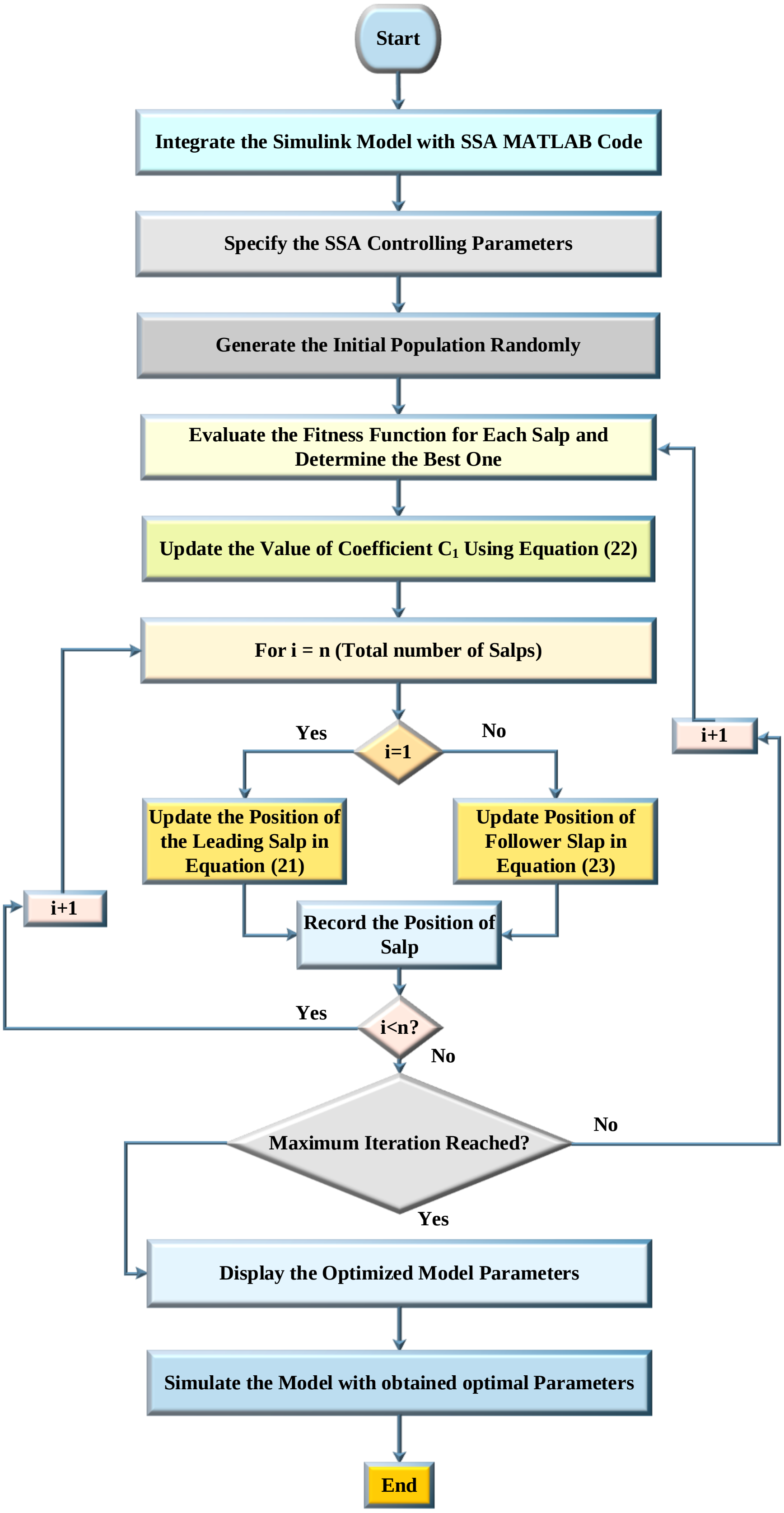

Figure 4. Flowchart of Salp Swarm Algorithm.

3.2. Fractional Order PID Controller

The use of fractional calculus was developed/increased when Podlubny proposed the $PI^{\lambda}D^{\mu}$ controller in 1999. This generality of the typical PID controller included a fractional integration of order λ and a fractional derivation of order μ, and it has since led numerous scholars to a new area of study called the modification of the fractional-order controller $PI^{\lambda}D^{\mu}$. Fractional order controllers are described using fractional calculus, where the calculus of proportional α—derivative is well-defined by the basic operator $\alpha^{D_t^\alpha}$, as mentioned in Equation (24).

$$\alpha^{D_t^\alpha} = \begin{Bmatrix} \frac{d^\alpha}{dt^\alpha}\ \alpha > 0 \\ 1\ \alpha = 0 \\ \int_\alpha^t (d\tau)^{-\alpha}\ \alpha < 0 \end{Bmatrix} \tag{24}$$

Upper and lower bounds are determined by α and t, while $\alpha \in \mathbb{R}$ and α operator can be substituted in the frequency domain as $F(s) = \frac{1}{S^\alpha}$. The output equation of the fractional-order controller in the time domain is given by Equation (25)

$$u = k_p e(t) + k_i D_t^{-\lambda} e(t) + k_d D_t^{\mu} e(t) \tag{25}$$

where, k_d is the differentiating constant, whereas k_i is the integration constant, and k_p is the proportional constant, μ is the fractional order of the differentiating action and λ is the fractional order of the integrating action.

In contrast to standard PID controllers, fractional-order controllers include two extra parameters that represent the order of integrating and derivative values, respectively. Based on the modification of these two factors, one can discover a wide range of fractional order controller choices.

As can be seen in Figure 5, the fractional order PI D controller expands the traditional PID controller from a point to a plane. The design of PID control may benefit greatly from this expansion's increased flexibility. Clearly, by selecting $[\lambda, \mu] = [1,\ 1]$, a traditional PID corrector can be regained; and by selecting $[\lambda, \mu] = [1,\ 0]$ and $[\lambda, \mu] = [0,\ 1]$, one can get traditional PI and PD controllers, respectively.

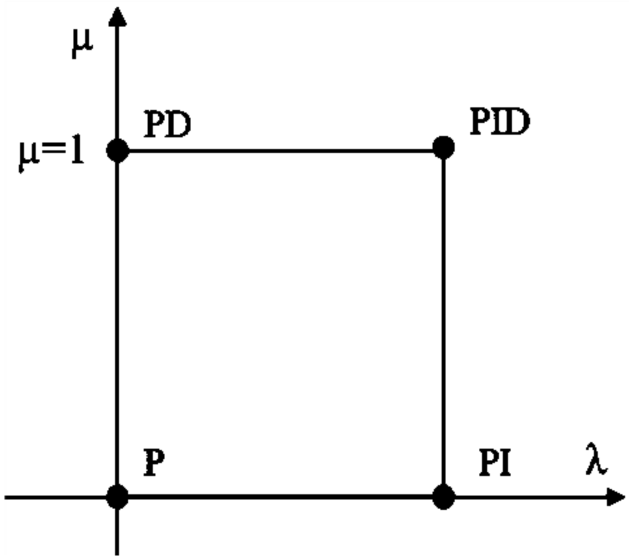

Figure 5. Types of Controllers According to Coefficients.

The FOPID executes much better than the traditional PID, since it uses discretized values. Moreover, as the stability region of the FOPID is wider than that of the PID controller, it is evident from Figure 6 that it enables more flexibility to the controller.

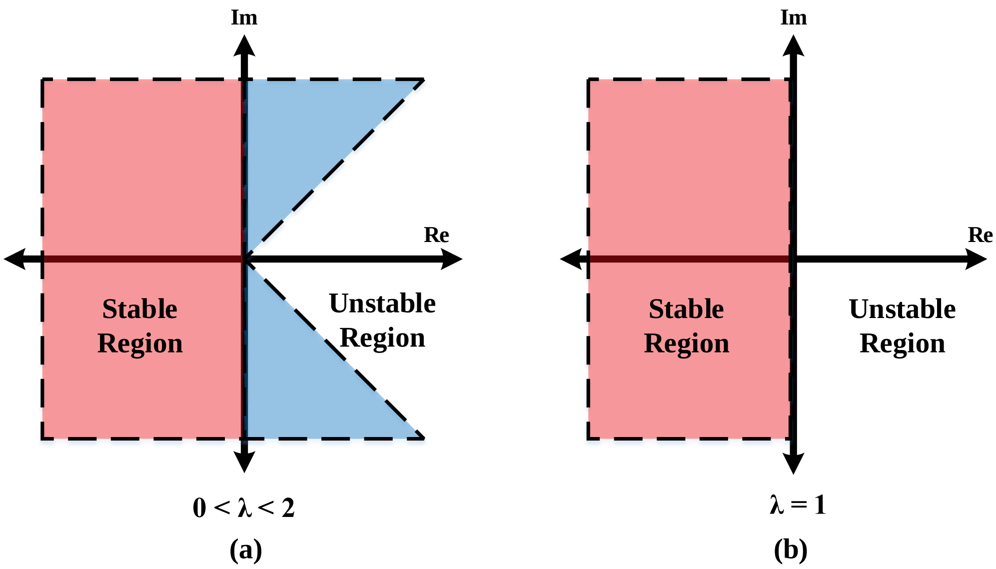

Figure 6. Stability Region of Controllers (**a**) FOPID (**b**) PID.

4. Results and Discussion

The hybrid system constituted of grid tied PEMFC and PV is simulated on MATLAB/Simulink for dynamic operation. The proposed FOPID controller is tested under different load conditions. Results are then compared with the conventional PI controller which substantiates the efficiency of the proposed (FOPID) controller.

Figure 7 depicts the change in irradiance, applied as input to PV to test the response of the controller, while Figure 8 shows the consumption of oxygen and hydrogen in the fuel cell. After the initial disturbance, the fuel consumption attains a constant value.

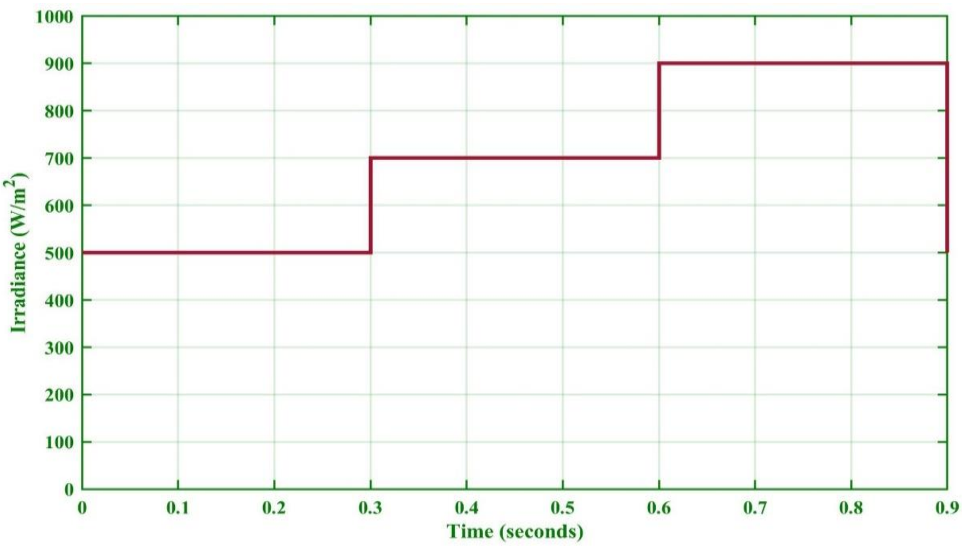

Figure 7. Abrupt Irradiance Change.

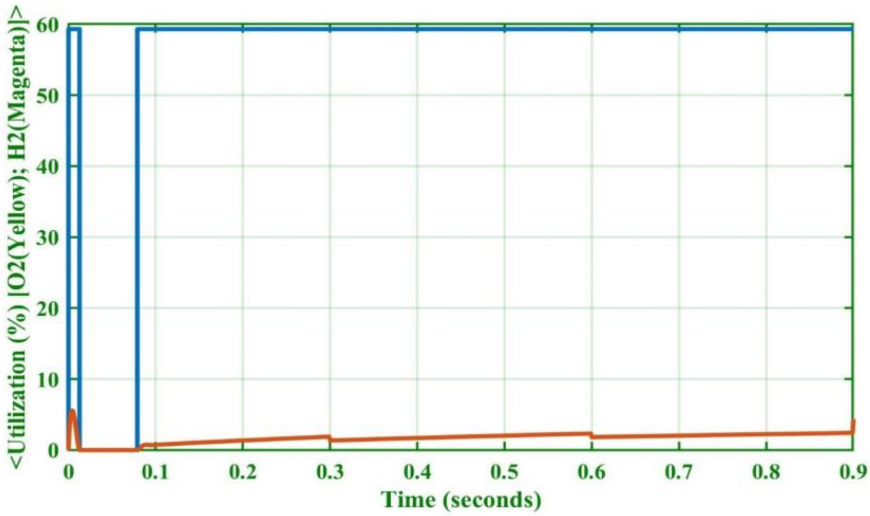

Figure 8. Oxygen and Hydrogen Consumption.

Figures 9 and 10 indicate the fuel cell output voltage and output current, respectively.

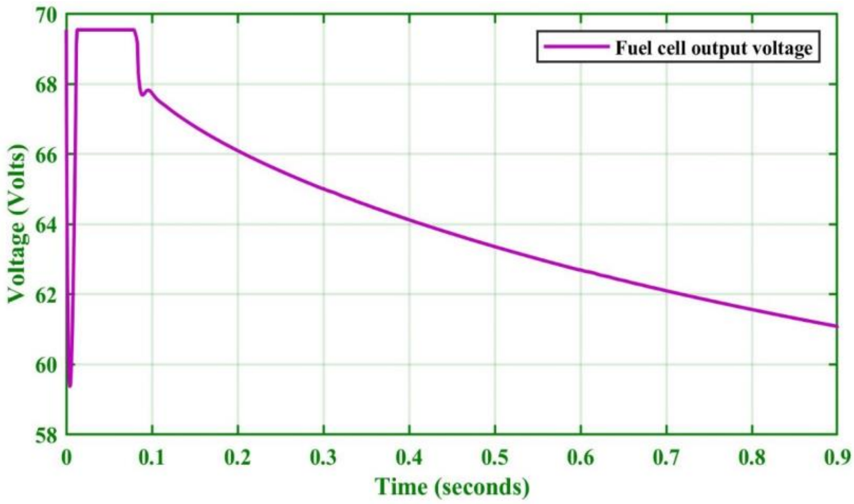

Figure 9. Fuel Cell Output Voltage.

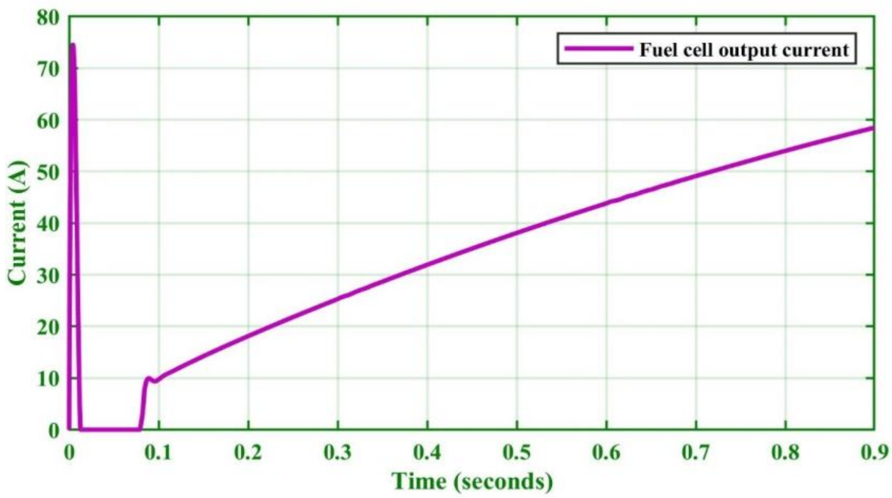

Figure 10. Fuel Cell Output Current.

The purpose of this research was to propose and test a robust control system that is effective under varying circumstances. The same was put to the test. Figure 11 shows the output current of the hybrid system using the conventional PI controller. Nevertheless, Figure 12 depicts the output current of the hybrid system using the proposed FOPID controller and a comparison is displayed with the conventional PI controller in Figure 13.

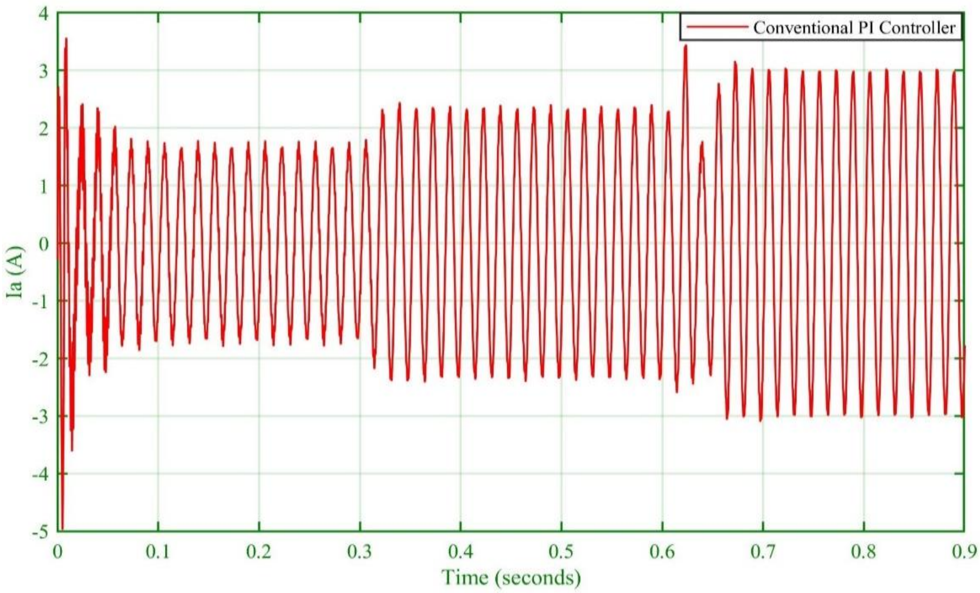

Figure 11. Output Current—Using Conventional PI.

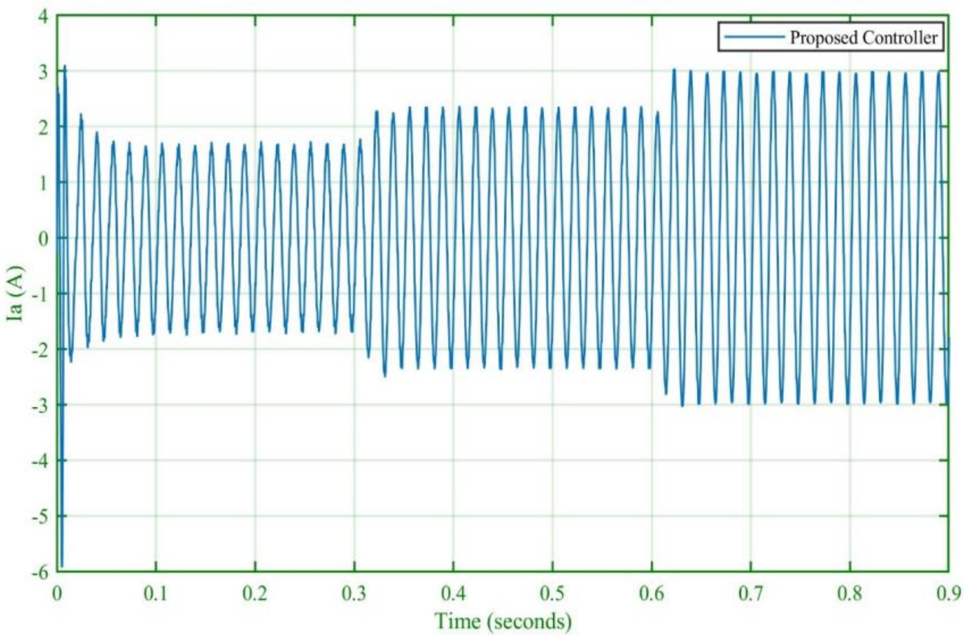

Figure 12. Output Current—Using Proposed Controller.

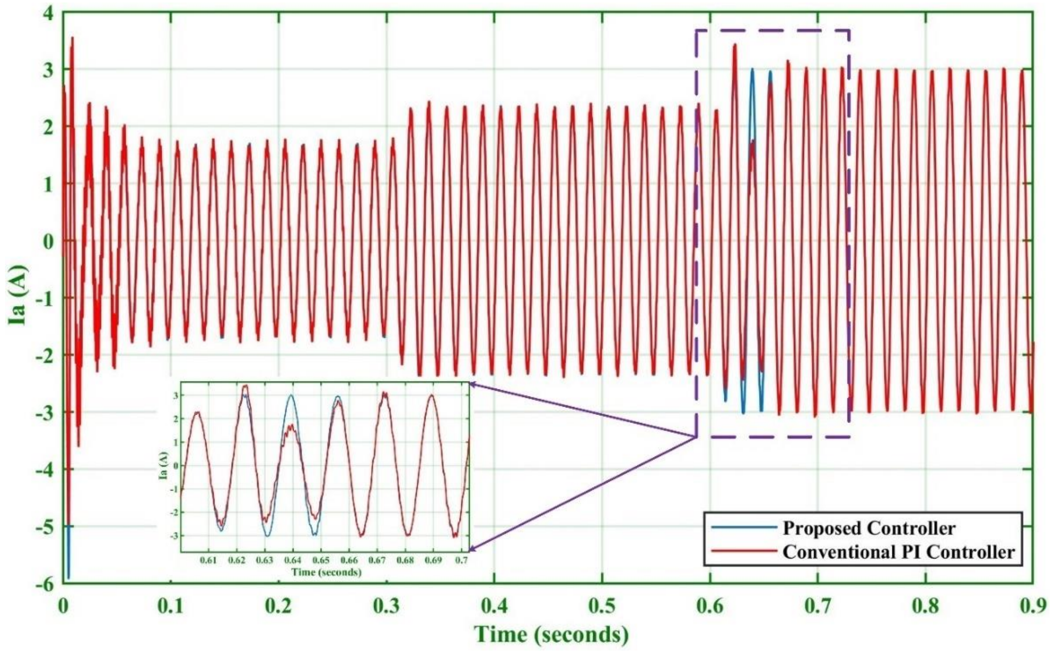

Figure 13. Output Current−Controller Comparison.

Figure 14 reveals the output power, for both controllers, and it is noticeable that the proposed FOPID controller shows significantly fewer oscillations and less settling time as compared to the conventional PI controller. DC output voltage (V_{dc}) is shown in Figure 15, which clearly indicates the superior performance of the projected controller and is more optimum against the uncertainties in the system.

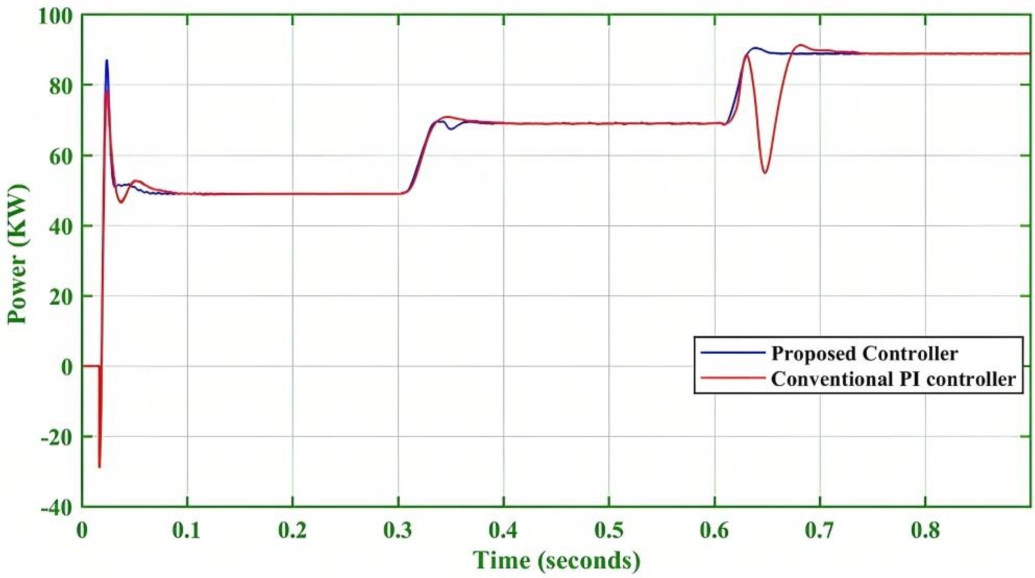

Figure 14. Output Power−Controller Comparison.

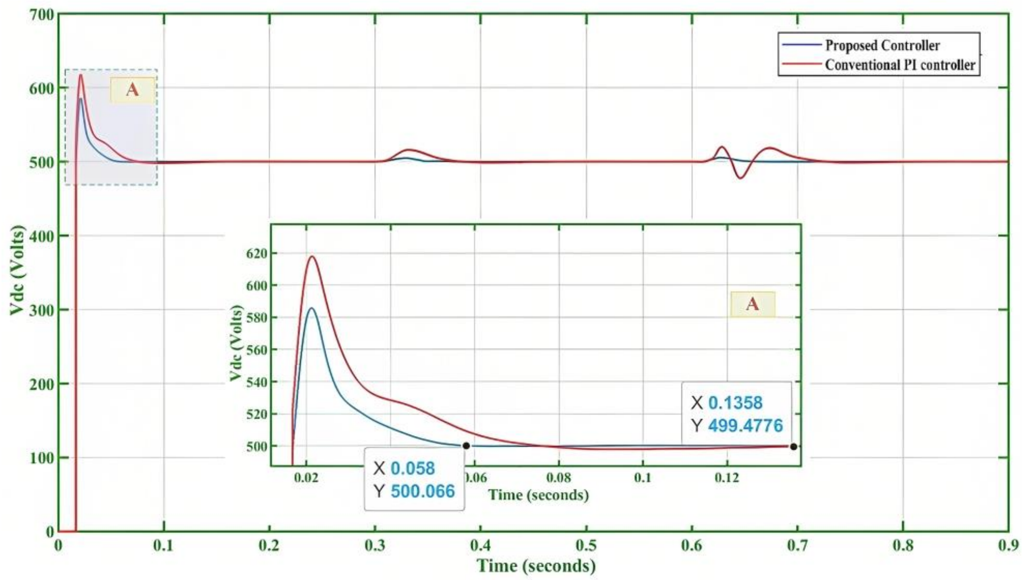

Figure 15. DC Output Voltage—Controller Comparaison.

5. Conclusions

This research work has presented a robust control strategy using optimum salp swarm algorithm tuned fractional order PID controller for the tracking of MPP of grid tied PEMFC along with PV. The proposed controller tracks the MPP whenever uncertainty of fluctuation occurs. Conventional P&O is used to control the duty cycle of the DC-DC converter, while FOPID controls the output of the DC-AC inverter. The overall capability of the suggested controller is significantly improved over the typical/conventional PI controller; and it offers high-power tracking capability, quick convergence speed, fewer controlling parameters, and ease of implementation. In the given test bench for abrupt irradiance change, the settling time is observed just 0.058 s with minimum overshoot, as compared to the conventional PI controller. Moreover, the overall suggested regulating technique adapts to the unforeseen power system scenario fairly successfully, with minimal oscillation.

Funding: This research was funded by the King Fahd University of Petroleum & Minerals, Dhahran 31261, Saudi Arabia.

Institutional Review Board Statement: Not applicable.

Informed Consent Statement: Not applicable.

Data Availability Statement: Not applicable.

Acknowledgments: This publication is based upon work supported by King Fahd University of Petroleum & Minerals. Author at KFUPM acknowledge the Interdisciplinary Research Center for Renewable Energy and Power Systems for the support received under Grant no. EC221008.

Conflicts of Interest: The author declares no conflict of interest.

References

1. Zheng, J.; Du, J.; Wang, B.; Klemeš, J.J.; Liao, Q.; Liang, Y. A hybrid framework for forecasting power generation of multiple renewable energy sources. *Renew. Sustain. Energy Rev.* **2023**, *172*, 113046. [CrossRef]
2. Harrabi, N.; Souissi, M.; Aitouche, A.; Chaabane, M. Modeling and control of photovoltaic and fuel cell based alternative power systems. *Int. J. Hydrogen Energy* **2018**, *43*, 11442–11451. [CrossRef]
3. Gulzar, M.M.; Iqbal, M.; Shahzad, S.; Muqeet, H.A.; Shahzad, M.; Hussain, M.M. Load Frequency Control (LFC) Strategies in Renewable Energy-Based Hybrid Power Systems: A Review. *Energies* **2022**, *15*, 3488. [CrossRef]
4. Mohamed, N.; Aymen, F.; Altamimi, A.; Khan, F.A.; Lassaad, S. Power Management and Control of a Hybrid Electric Vehicle Based on Photovoltaic, Fuel Cells, and Battery Energy Sources. *Sustainability* **2022**, *14*, 2551. [CrossRef]

5. Javed, M.Y.; Gulzar, M.M.; Rizvi, S.T.H.; Arif, A. A hybrid technique to harvest maximum power from PV systems under partial shading conditions. In Proceedings of the 2016 International Conference on Emerging Technologies (ICET), Islamabad, Pakistan, 18–19 October 2016; IEEE: Manhattan, NY, USA, 2016; pp. 1–5.
6. Mohamed, A.; Peer, K.R.M.; Chandrakala, V.; Saravanan, S. Comparative study of maximum power point tracking techniques for fuel cell powered electric vehicle. In Proceedings of the IOP Conference Series: Materials Science and Engineering, Wuhan, China, 10–12 October 2019; IOP Publishing: Bristol, UK, 2019; Volume 577, No. 1. p. 012031.
7. Luta, D.N.; Raji, A.K. Fuzzy rule-based and particle swarm optimisation MPPT techniques for a fuel cell stack. *Energies* **2019**, *12*, 936. [CrossRef]
8. Reddy, K.J.; Sudhakar, N. ANFIS-MPPT control algorithm for a PEMFC system used in electric vehicle applications. *Int. J. Hydrogen Energy* **2019**, *44*, 15355–15369. [CrossRef]
9. Rezk, H.; Fathy, A. Performance improvement of PEM fuel cell using variable step-size incremental resistance MPPT technique. *Sustainability* **2020**, *12*, 5601. [CrossRef]
10. Derbeli, M.; Charaabi, A.; Barambones, O.; Napole, C. High-performance tracking for proton exchange membrane fuel cell system pemfc using model predictive control. *Mathematics* **2021**, *9*, 1158. [CrossRef]
11. Saleh, B.; Yousef, A.M.; Abo-Elyousr, F.K.; Mohamed, M.; Abdelwahab, S.A.M.; Elnozahy, A. Performance Analysis of Maximum Power Point Tracking for Two Techniques with Direct Control of Photovoltaic Grid-Connected Systems. *Energy Sources Part A Recovery Util. Environ. Eff.* **2022**, *44*, 413–434. [CrossRef]
12. Hanan, M.; Ai, X.; Javed, M.Y.; Gulzar, M.M.; Ahmad, S. A two-stage algorithm to harvest maximum power from photovoltaic system. In Proceedings of the 2018 2nd IEEE Conference on Energy Internet and Energy System Integration (EI2), Beijing, China, 20–22 October 2018; IEEE: Manhattan, NY, USA, 2018; pp. 1–6.
13. Wang, M.H.; Huang, M.; Jiang, W.; Liou, K.-J. Maximum power point tracking control method for proton exchange membrane fuel cell. *IET Renew. Power Gener.* **2016**, *10*, 908–915. [CrossRef]
14. Nasiri, A.I.; Sarvi, M. A new maximum power point tracking method for PEM fuel cells based on water cycle algorithm. *J. Renew. Energy Environ.* **2016**, *3*, 35–42.
15. Rezk, H. Performance of incremental resistance MPPT based proton exchange membrane fuel cell power system. In Proceedings of the 2016 Eighteenth International Middle East Power Systems Conference (MEPCON), Cairo, Egypt, 27–29 December 2016; IEEE: Manhattan, NY, USA, 2016; pp. 199–205.
16. Derbeli, M.; Sbita, L.; Farhat, M.; Barambones, O. Proton exchange membrane fuel cell—A smart drive algorithm. In Proceedings of the 2017 International Conference on Green Energy Conversion Systems (GECS), Hammamet, Tunisia, 23–25 March 2017; IEEE: Manhattan, NY, USA, 2017; pp. 1–5.
17. Ahmadi, S.; Abdi, S.; Kakavand, M. Maximum power point tracking of a proton exchange membrane fuel cell system using PSO-PID controller. *Int. J. Hydrogen Energy* **2017**, *42*, 20430–20443. [CrossRef]
18. Liu, J.; Zhao, T.; Chen, Y. Maximum power point tracking with fractional order high pass filter for proton exchange membrane fuel cell. *IEEE/CAA J. Autom. Sin.* **2017**, *4*, 70–79. [CrossRef]
19. Priyadarshi, N.; Sharma, A.K.; Azam, F. A hybrid firefly-asymmetrical fuzzy logic controller based MPPT for PV-wind-fuel grid integration. *Int. J. Renew. Energy Res.* **2017**, *7*, 1546–1560.
20. Derbeli, M.; Barambones, O.; Sbita, L. A robust maximum power point tracking control method for a PEM fuel cell power system. *Appl. Sci.* **2018**, *8*, 2449. [CrossRef]
21. Fan, L.; Ma, X. Maximum power point tracking of PEMFC based on hybrid artificial bee colony algorithm with fuzzy control. *Sci. Rep.* **2022**, *12*, 4316. [CrossRef]
22. Sibtain, D.; Gulzar, M.M.; Shahid, K.; Javed, I.; Murawwat, S.; Hussain, M.M. Stability Analysis and Design of Variable Step-Size P&O Algorithm Based on Fuzzy Robust Tracking of MPPT for Standalone/Grid Connected Power System. *Sustainability* **2022**, *14*, 8986.
23. Attia, H.; Hossin, K. Efficient maximum power point tracker based on neural network and sliding-mode control for buck converters. *Clean Energy* **2022**, *6*, 716–725. [CrossRef]
24. Priyadarshi, N.; Padmanaban, S.; Bhaskar, M.S.; Blaabjerg, F.; Holm-Nielsen, J.B.; Azam, F.; Sharma, A.K. A hybrid photovoltaic-fuel cell-based single-stage grid integration with Lyapunov control scheme. *IEEE Syst. J.* **2019**, *14*, 3334–3342. [CrossRef]
25. Rana, K.P.S.; Kumar, V.; Sehgal, N.; George, S. A novel dPdI feedback based control scheme using GWO tuned PID controller for efficient MPPT of PEM fuel cell. *ISA Trans.* **2019**, *93*, 312–324. [CrossRef]
26. Fathy, A.; Abdelkareem, M.A.; Olabi, A.; Rezk, H. A novel strategy based on salp swarm algorithm for extracting the maximum power of proton exchange membrane fuel cell. *Int. J. Hydrogen Energy* **2021**, *46*, 6087–6099. [CrossRef]
27. Belhaj, F.Z.; El Fadil, H.; El Idrissi, Z.; Koundi, M.; Gaouzi, K. Modeling, Analysis and Experimental Validation of the Fuel Cell Association with DC-DC Power Converters with Robust and Anti-Windup PID Controller Design. *Electronics* **2020**, *9*, 1889. [CrossRef]
28. Qi, Z.; Tang, J.; Pei, J.; Shan, L. Fractional controller design of a DC-DC converter for PEMFC. *IEEE Access* **2020**, *8*, 120134–120144. [CrossRef]
29. Derbeli, M.; Barambones, O.; Farhat, M.; Ramos-Hernanz, J.A.; Sbita, L. Robust high order sliding mode control for performance improvement of PEM fuel cell power systems. *Int. J. Hydrogen Energy* **2020**, *45*, 29222–29234. [CrossRef]
30. Silaa, M.Y.; Derbeli, M.; Barambones, O.; Cheknane, A. Design and Implementation of High Order Sliding Mode Control for PEMFC Power System. *Energies* **2020**, *13*, 4317. [CrossRef]
31. Derbeli, M.; Barambones, O.; Silaa, M.Y.; Napole, C. Real-Time Implementation of a New MPPT Control Method for a DC-DC Boost Converter Used in a PEM Fuel Cell Power System. *Actuators* **2020**, *9*, 105. [CrossRef]

32. Gulzar, M.M.; Sibtain, D.; Ahmad, A.; Javed, I.; Murawwat, S.; Rasool, I.; Hayat, A. An Efficient Design of Adaptive Model Predictive Controller for Load Frequency Control in Hybrid Power System. *Int. Trans. Electr. Energy Syst.* **2022**, *2022*, 7894264. [CrossRef]
33. Gulzar, M.M.; Rizvi, S.T.H.; Javed, M.Y.; Sibtain, D.; Din, R.S.U. Mitigating the load frequency fluctuations of interconnected power systems using model predictive controller. *Electronics* **2019**, *8*, 156. [CrossRef]
34. Fathy, A.; Alharbi, A.G.; Alshammari, S.; Hasanien, H.M. Archimedes optimization algorithm based maximum power point tracker for wind energy generation system. *Ain Shams Eng. J.* **2022**, *13*, 101548. [CrossRef]
35. Silaa, M.Y.; Derbeli, M.; Barambones, O.; Napole, C.; Cheknane, A.; De Durana, J.M.G. An efficient and robust current control for polymer electrolyte membrane fuel cell power system. *Sustainability* **2021**, *13*, 2360. [CrossRef]
36. Bahri, H.; Harrag, A. Ingenious golden section search MPPT algorithm for PEM fuel cell power system. *Neural Comput. Appl.* **2021**, *33*, 8275–8298. [CrossRef]
37. Fathy, A.; Rezk, H.; Alanazi, T.M. Recent approach of forensic-based investigation algorithm for optimizing fractional order PID-based MPPT with proton exchange membrane fuel cell. *IEEE Access* **2021**, *9*, 18974–18992. [CrossRef]
38. Kraiem, H.; Flah, A.; Mohamed, N.; Messaoud, M.H.B.; Al-Ammar, E.A.; Althobaiti, A.; Alotaibi, A.A.; Jasiński, M.; Suresh, V.; Leonowicz, Z.; et al. Decreasing the Battery Recharge Time if Using a Fuzzy Based Power Management Loop for an Isolated Micro-Grid Farm. *Sustainability* **2022**, *14*, 2870. [CrossRef]
39. Rezk, H.; Aly, M.; Fathy, A. A novel strategy based on recent equilibrium optimizer to enhance the performance of PEM fuel cell system through optimized fuzzy logic MPPT. *Energy* **2021**, *234*, 121267. [CrossRef]
40. Xie, M.; Gulzar, M.M.; Tehreem, H.; Xie, M.; Javed, M.Y.; Rizvi, S.T.H. Automatic Voltage Regulation of Grid Connected Photovoltaic System Using Lyapunov Based Sliding Mode Controller: A Finite-Time Approach. *Int. J. Control Autom. Syst.* **2020**, *18*, 1550–1560. [CrossRef]
41. Iqbal, M.; Gulzar, M.M. Master-slave design for frequency regulation in hybrid power system under complex environment. *IET Renew. Power Gener.* **2022**, *16*, 3041–3057. [CrossRef]